A Communication-Based Appliance Scheduling Scheme for Consumer-Premise Energy Management Systems

Journal:	*IEEE Transactions on Smart Grid*
Manuscript ID:	Draft
Manuscript Type:	Special Issue: Smart Grid Communication Systems: Reliability, Dependability & Performance
Date Submitted by the Author:	n/a
Complete List of Authors:	Chen, Chen; Lehigh University, Electrical and Computer Engineering Nagananda, Kyatsandra; Lehigh University, Electrical and Computer Engineering Xiong, Gang; Intel Corporation, Kishore, Shalinee; Lehigh University, Electrical and Computer Engineering Snyder, Lawrence; Lehigh University, Industrial and Systems Engineering
Technical Topic Area :	Communication and control in energy systems < Transactions on Smart Grid, Energy Management Systems < Transactions on Smart Grid
Key Words:	Demand Response, Scheduling, Delay, Distributed Wind Power

A Communication-Based Appliance Scheduling Scheme for Consumer-Premise Energy Management Systems

Chen Chen, K.G. Nagananda, Gang Xiong, Shalinee Kishore, *Member, IEEE* and Lawrence V. Snyder, *Member, IEEE*

***Abstract*—In this paper, a communication-based load scheduling protocol is proposed for in-home appliances connected over a home area network. Specifically, a joint access and scheduling approach for appliances is developed to enable in-home appliances to coordinate power usage so that the total energy demand for the home is kept below a target value. The proposed protocol considers both "schedulable" appliances which have delay flexibility, and "critical" appliances which consume power as they desire. An optimization problem is formulated for the energy management controller to decide the target values for each time slot, by incorporating the variation of electricity prices and distributed wind power uncertainty. We model the evolution of the protocol as a two-dimensional Markov chain, and derive the steady-state distribution, by which the average delay of an appliance is then obtained. Simulation results verify the analysis and show cost saving to customers using the proposed scheme.**

***Index Terms*—Demand Response, Scheduling, Delay, Distributed Wind Power**

I. Introduction

PEAK demand hours, which happen for only a portion of time in any given year, renders the existing U.S. power grid less efficient. For example, 10% of all generation assets and 25% of distribution infrastructure are required for less than 400 hours per year, roughly 5% of the time [1]. One way to overcome this inefficiency is to modify demand, particularly during peak hours, which is the focus of *demand response* (DR) programs.

Future DR efforts will be enhanced by emerging *smart grid* infrastructure which provides greater information, flexibility and control to electricity suppliers, grid operators, and end-use consumers. A key feature of the smart grid is the smart meter which facilitates real-time information exchange between electricity service providers and their customers. One way in which service providers may influence consumer demand is to use the metering infrastructure to deliver "real-time" electricity prices, *e.g.*, once every fifteen minutes. The extent to which these time-varying prices may make overall demand more controllable (especially during peak hours) depends greatly on the consumer's ability to quickly and effectively respond to such pricing signals. Thus an equally important component of this DR approach is an *energy management controller* that incorporates prices and user preferences to provide consumers with electricity usage options that can save them money (presumably by curtailing loads during or shifting loads away from peak hours).

In the residential scenario, the EMC can make decisions for a particular residence or for a demand response aggregator which combines controllable loads from a collection of residences. In either case, we refer to the operating space of the EMC as the *consumer premise*, where the consumer could be and individual homeowner or an aggregator. In making these decisions, the EMC can decide to curtail loads or it can take advantage of the flexibility of certain types of appliances to change their load profiles. For instance, some appliances offer flexibility in the operation time (*e.g.*, dish washer or clothes washer/dryer) so that their start-time can be delayed under the constraint of a hard deadline. An important emerging class of appliances that provides even more flexibility in their power draw is electric vehicles (EVs); the power consumption of EVs can be modified as long as the total energy requirement is fulfilled by a given deadline. Such load shifting benefits both the grid and customers. From the grid's perspective, the reduced peak demand 1) lowers the cost of employing less-efficient generation; 2) alleviates transmission congestion; and 3) helps maintain grid stability during these critical peak hours. From the customer's perspective, shifting load to off-peak periods results in reduced electricity bills and occurrences of blackouts and brownouts.

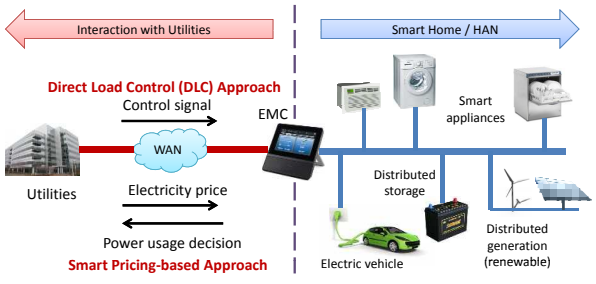

Fig. 1. The consumer-premise energy management system

When implemented at the aggregate level, the EMC is directly controlling loads in individual residences and is thus participating in some type of *direct load control* (DLC),

C. Chen, K.G. Nagananda, and S. Kishore are with the Department of Electrical and Computer Engineering, Lehigh University, Bethlehem, PA 18015 USA (e-mail: {cchen,kgn209,skishore}@lehigh.edu)

L. V. Snyder is with the Department of Industrial and Systems Engineering, Lehigh University, Bethlehem, PA 18015 USA (e-mail:lvs2@lehigh.edu)

G. Xiong is with Intel Corporation, Portland, OR USA (e-mail: gxiong@lehigh.edu)

Manuscript received March 31, 2012.

shown in Fig. 1. In such cases, individual homeowners make contractual agreements with a demand response aggregator (which could be a utility) which permits the aggregator to remotely control operations and energy consumption of certain appliances within the household. An aggregator with this scheduling ability can participate in the wholesale electricity markets as a DR resource [2], [3]. Most existing DLC programs issued by Independent System Operators (ISOs) are based on load curtailment; that is, the DR aggregator (*i.e.*, their EMCs) must make decisions about which loads to turn off during peak hours. Aside from being intrusive, these load curtailment solutions (which control each appliance directly) imply high communication complexity and must often deal with energy pay-back or load recovery. In [4], a DR mechanism is proposed in which the aggregator can further adaptively delay loads over a collection of households in a scalable manner. While this approach alleviates other shortcomings of existing DLC schemes, it is still an intrusive mechanism.

When EMCs operate in individual homes, the underlying DR mechanism is based on smart pricing, also shown in Fig. 1. In this scheme, residential customers are encouraged to individually and voluntarily manage their loads by means of some type of a time-varying price profile. The time-variable pricing can be either critical-peak pricing (CPP), time-of-use pricing (TOU), or real-time pricing (RTP). Based on these price profiles, the EMC (acting on behalf of the customer) can shift or change their power consumption with the goal to meet user preferences (*e.g.*, meet deadlines) while saving money. This scheme can bring wholesale price variations into the retail market and can be implemented by an aggregator/utility. Until now, only certain types of these schemes have been implemented in the residential setting [5], [6] but have recently gained a lot of attention. While this approach does not surrender control of appliances to entities outside the home, it has its own shortcomings. This includes calculation of stable pricing policies, ensuring timely delivery of these prices, and the wariness of customers towards price uncertainty.

Besides improving demand side management, the role of the EMC also involves managing and making better use of local renewable distributed energy resources (DERs). Existing regulations incentivize residential and small business consumers to install renewable resources like solar panels and wind turbines [7]. Several products and installation services of residential renewable DER are also currently available [8]. As the penetration of these devices increases, the customers using them will become increasingly interested in how to best manage the local electricity supply and demand in the face of future pricing based DR mechanisms.

In this paper, we focus on how a consumer premise communication network can be designed to permit load scheduling amongst flexible and controllable loads. The functionalities of the EMC are reduced in our model to calculating a threshold maximum power consumption for the premise (*e.g.*, the home). We present the calculation of this time-varying threshold power as an optimization which accounts for price variation and uncertainty due to local wind generation. Our proposed joint access and scheduling protocol describes how appliances access a common control channel so that this total maximum demand target is not exceeded for each time slot. The evolution of the protocol is modeled as a two-dimensional Markov chain. The average delay for an appliance can then be obtained from its steady state distribution. Unlike existing local area network (LAN) media access protocols (*e.g.*, Wi-Fi, G.hn, Zigbee), which could be used for one of several applications, our proposed scheme specifically addresses the load control problem. For in-home scenarios, relatively short control messages are occasionally exchanged; thus the approach can be easily implemented on higher data-rate LANs (such as those listed above) that support other applications as long as the load control messages are given transmission priority.

We also note that although we have framed our protocol for an individual consumer premise (*i.e.*, one in which an in-home EMC converts time-varying prices and local generation to time-varying threshold power levels), the proposed scheme could be also be used in aggregate programs (*e.g.*, as an alternative to existing DLC-type programs). Here, the utility/aggregator decides the target value for each home by optimizing its own cost function.[1] The in-home appliances can then use the proposed packet exchange algorithms to stay within the target value. The result is an aggregate scheme that is less intrusive (*e.g.*, preserves privacy of the individual homeowner); and since the control tasks are conducted in a distributed way, communication complexity is no longer an issue.

Finally, we note that unlike existing studies on EMC design (*e.g.*, [9], [10], [11], [12]), the energy management approach presented here is tightly coupled with the underlying communication algorithm among the appliances. Initial results of this work have been presented in [13], [14]. In this paper, we additionally formulate the EMC's optimization of the target power value that accounts for both price variation and distributed wind power uncertainty. To do so, we employ the Markov Chain Monte Carlo (MCMC) method to describe the stochastic property of power generation from wind turbines. Simulation results verify our analysis and show customers' savings using this proposed scheme.

The remainder of the paper is organized as follows. Section II describes the joint access and scheduling scheme of the appliances. Section III derives the average delay of an appliance for this scheme using the Markov chain model. Section IV formulates the EMC optimization for the target power. Section V provides numerical results and we conclude our discussion in Section VI.

II. Access and Scheduling Scheme for Appliances

A. Protocol Description

We assume a HAN with N appliances that share a common control channel. Time is segmented into *scheduling frames*, which are of the order of several (*e.g.*, 5) minutes, and there may be multiple scheduling frames in the duration between pricing updates. Due to the long frame and short packet

[1]This calculation can again be done by an aggregate level EMC using our proposed optimization,

durations in the proposed scheme, we assume that collisions occur on the control channel with negligible probability.

We define the *active set* ($\mathcal{A}_t$) as the set of appliances which are operating during time t. We also assign a *leader* appliance (ℓ_t) that broadcasts beacon signals and makes admission control decisions during time t. In a centralized scheme, the EMC could be the (static) leader; or in a distributed scheme, any one of the appliances in $\mathcal{A}_t$ can be the leader. Later in this section, we present a possible leader assignment approach. Two types of appliances are considered in the home:

1) *Critical appliances*, that must join $\mathcal{A}_t$ immediately. Examples include lighting, medical devices, laptops, TV, *etc*.
2) *Schedulable appliances*, that can be powered on with a tolerable delay.

We first consider the case with only schedulable appliances and then discuss modifications to include critical appliances. Fig. 2 shows the frame structure of the proposed media-access and scheduling protocol. The frame consists of three phases: power update, power request and power scheduling, with duration T_1, T_2 and T_3, respectively.

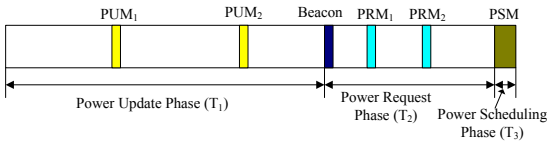

Fig. 2. Frame structure of proposed protocol

1) Power Update Phase (T_1): Any active appliance which finishes its power usage sends a power update message (PUM) packet, indicating the amount of power the appliance is releasing. Any appliance that completes operation during the other two phases waits until the next power update phase to transmit the PUM packet. At the end of the power update phase, the leader appliance ℓ_t calculates the remaining power budget:

$$\mathcal{P}_r^{(t)} = \mathcal{P}_{\max,t} - \sum_{j\in\mathcal{A}_t} \mathcal{P}_j, \tag{1}$$

where $\mathcal{P}_r^{(t)}$ is the remaining power at time t, $\mathcal{P}_{\max,t}$ is the total demand target value and $\mathcal{P}_j$ is the power usage for an appliance j when on. The leader then broadcasts this information in the beacon signal, which marks the start of the second phase.

2) Power Request Phase (T_2): This phase is divided into time slots. In the first slot, the leader appliance sends out a beacon signal indicating the remaining power budget $\mathcal{P}_r^{(t)}$. Any (schedulable) appliance, i, which wishes to join the active set listens to the control channel and, upon receiving the leader's beacon signal, compares its requested power level with the remaining power budget. If its requested demand exceeds the remaining power budget, i.e., $\mathcal{P}_i \geq \mathcal{P}_r^{(t)}$, then appliance i will defer requesting access to the active set until the next time frame. Otherwise, it attempts joining the active set in the current frame. Appliances that pass this "power check" enter into the *feasible appliance set* ($\mathcal{F}_t$).

In order to be scheduled to power on, each appliance in $\mathcal{F}_t$ waits for a random number of time slots (uniformly distributed over $[1, w]$, where w is the number of slots in this phase), and then sends out a power request message (PRM) packet to request the power usage. Appliances in $\mathcal{F}_t$ whose PRM packets are received correctly by the leader enter into the *admissible appliance set* ($\mathcal{D}_t$). During this time, the leader monitors the control channel and collects all the power request information.

3) Power Scheduling Phase (T_3): During this phase, the leader appliance makes an admission control decision, *i.e.*, decides which (schedulable) appliances in $\mathcal{D}_t$ can join the active set. These appliances form the *newly admitted appliance set* ($\mathcal{N}_t$). Several admission control methods will be discussed later in this section. The leader then broadcasts a power scheduling message (PSM) packet, heard by all (including active) appliances. Upon reception of the PSM packet, the appliances in $\mathcal{N}_t$ start consuming power immediately. Any non-admitted appliances will wait until next frame to request again. The format of PUM, PRM, and PSM packets is detailed in [13].

In the case that there is no EMC in the home (*e.g.*, if the aggregator/utility determines the target power and send this to the home), the first appliance which powers on will be the leader and sends out the beacon signal to synchronize all appliances in the system. Subsequently, the last admitted appliance (the one listed last in the PSM message) is the leader for the upcoming frame. Thus, the role of the leader could potentially change from one frame to the next.

B. Admission Control Methods (ACM)

When the total request power is greater than the remaining power budget, *i.e.*, $\sum_{i\in\mathcal{D}_t} \mathcal{P}_i \geq \mathcal{P}_{\max,t} - \sum_{j\in\mathcal{A}_t} \mathcal{P}_j$, the leader appliance makes an admission decision. We consider the following ACMs, though others are possible:

1) Random ACM: The leader appliance randomly removes appliances from the admissible set $\mathcal{D}_t$ to meet $\mathcal{P}_{\max,t}$:

Step 1: Randomly remove appliance i from $\mathcal{D}_t$. Let $\mathcal{D}_t = \mathcal{D}_t \backslash \{i\}$ and calculate $\mathcal{P}_l = \sum_{i\in\mathcal{D}_t\cup\mathcal{A}_t} \mathcal{P}_i - \mathcal{P}_{\max,t}$.

Step 2: If $\mathcal{P}_l \leq 0$, set $\mathcal{N}_t = \mathcal{D}_t$ and stop; else go to Step 1.

2) Max-Power Oriented ACM: The leader appliance maximizes the total additional power supported without exceeding the remaining power budget:

$$\begin{aligned} \max_{x_i} \quad & \sum_{i\in\mathcal{D}_t} x_i\mathcal{P}_i \\ \text{s.t.} \quad & \sum_{i\in\mathcal{D}_t} x_i\mathcal{P}_i \leq \mathcal{P}_{\max,t} - \sum_{j\in\mathcal{A}_t} \mathcal{P}_j \\ & x_i \in \{0,1\}. \end{aligned} \tag{2}$$

This is a classical $0-1$ knapsack problem, and can be solved using various existing approaches, *e.g.*, [15]. The newly admitted set can be chosen as $\mathcal{N}_t = \{i | x_i = 1,\ i \in \mathcal{D}_t\}$.

3) Max-Appliance Oriented ACM: The leader appliance selects in a way to support maximum number of appliances:

$$\begin{aligned} \max_{x_i} \quad & \sum_{i\in\mathcal{D}_t} x_i \\ \text{s.t.} \quad & \sum_{i\in\mathcal{D}_t} x_i\mathcal{P}_i \le \mathcal{P}_{\max,t} - \sum_{j\in\mathcal{A}_t}\mathcal{P}_j \\ & x_i \in \{0,1\}. \end{aligned} \tag{3}$$

The optimization problem in (3) can be solved by first sorting the requested power of individual appliances in an ascending order. Without loss of generality, we assume that $\mathcal{P}_1 \le \mathcal{P}_2 \le \cdots \le \mathcal{P}_{|\mathcal{D}_t|}$, where $|\cdot|$ denotes the cardinality of a set. Then,

$$\mathcal{N}_t = \left\{ \{1,\cdots,\max\{i_{\mathcal{S}}\}\} \middle| \sum_{k=1}^{i_{\mathcal{S}}} \mathcal{P}_k \le \mathcal{P}_{\max,t} - \sum_{j\in\mathcal{A}_t}\mathcal{P}_j \right\}.$$

C. Critical Appliance Consideration

When a critical appliance has a power request, it starts operating immediately and sends out PRM packets over the control channel. If there is sufficient power budget to support this appliance, the leader simply needs to adjust the remaining power level for use in admission control. Since all active appliances have access to the control channel, they too can update their measurement of the remaining power to account for the critical appliance's power usage.

On the other hand, if there is not enough remaining power to accommodate the current usage, then the leader must employ a *curtailment control method* (CCM). Towards this end, the leader constructs the *curtailable appliance set* ($\mathcal{C}_t$) from the active set at each time t. If $\mathcal{C}_t \neq \emptyset$, the leader selects a member of $\mathcal{C}_t$ that needs to be removed from $\mathcal{A}_t$. Similar to ACM, the CCM adopted by the leader has three criteria: *random curtailment*; *min-power curtailment*; and *min-appliance curtailment*. The reader is referred to [13] for details, where we also discussed the case when $\mathcal{C}_t = \emptyset$, and modification of the protocol when adding deadlines to the appliances.

We would also like to make a note about dynamic appliances (*e.g.*, heating-cooling systems). It is possible to consider these appliances as critical under our current model. Alternatively, we could consider them as a third category of appliances, which are critical in that they need to be on during a hot summer day but offer some degree of flexibility in terms of how often and how long they turn on/off. Modeling them as a third category of appliance would make for more efficient schedules since they would incorporate their load patterns when making admission/curtailment decisions. The resulting optimization would, however, be far more complicated. To keep this paper more focused, we exclude such extensions from our discussions here.

III. Markov Chain Analysis of the Protocol

In this section, we analyze the delay performance of the proposed joint access and scheduling protocol for appliances, by modeling the stochastic behavior of the protocol as a two-dimensional discrete-time Markov chain, and deriving its stationary distribution. First, we define some additional appliance sets as follows:

$\mathcal{R}_t$: *Released appliance set*, comprising appliances that release power (indicating completion of usage cycle) during time t;

$\mathcal{J}_t$: *Joining appliance set*, consisting of appliances that wish to join $\mathcal{A}_t$ during time t;

$\mathcal{I}_t$: *Arrival appliance set*, which contain appliances that request to power-on during time t.

A. Power Usage Statistic

We assume a finite number L of power levels for all appliances. Let ε_l denote the l-th power level, and without loss of generality we assume $\varepsilon_l = l\varepsilon$. Appliances' power draws are assumed to be random, with probability mass function (PMF) for appliance with power level $\mathcal{P} = l\varepsilon$ as

$$p_l \triangleq \Pr(\mathcal{P} = l\varepsilon).$$

For a set of ω appliances and each appliance with power usage $\mathcal{P}_i$, let $\mathcal{P}_\Sigma = \sum_{i=1}^{\omega}\mathcal{P}_i$ denote the overall power usage of appliances. Then the PMF of $\mathcal{P}_\Sigma$ can be written as

$$\phi_\Sigma(\omega, l_0) \triangleq \Pr(\mathcal{P}_\Sigma = l_0\varepsilon) = \sum_{\Omega} p_{l_1}\cdot p_{l_2}\cdots p_{l_\omega}, \tag{4}$$

where

$$\Omega = \left\{ (l_1,\ldots,l_\omega) \in \mathbb{L}^\omega \middle| \sum_{i=1}^{\omega} l_i = l_0,\ \mathbb{L} = \{1,\ldots,L\} \right\},$$
$$l_0 \in \{\omega, \omega+1, \cdots, \omega L\}.$$

The cumulative distribution function (CDF) of $\mathcal{P}_\Sigma$ is, therefore, given by

$$\Pr\Big(\mathcal{P}_\Sigma \le \bar{\mathcal{P}}\Big) = \sum_{l_0=\omega}^{\lfloor \bar{\mathcal{P}}/\varepsilon \rfloor} \phi_\Sigma(\omega, l_0). \tag{5}$$

B. Two-dimensional Discrete-time Markov Chain Model

Define the state $S(t) = \{|\mathcal{A}_t|, |\mathcal{J}_t| \big| |\mathcal{A}_t| + |\mathcal{J}_t| \le N\}$, for time slot t, indicating the number of active appliances and the number of appliances that wish to power on, respectively. The evolution of $S(t)$ can be modeled as two-dimensional discrete-time Markov chain. From the structure of the protocol (see Fig. 2), we have

$$\begin{aligned} &\mathcal{A}_t = \mathcal{A}_{t-1} \cup \mathcal{N}_{t-1} \backslash \mathcal{R}_t \Rightarrow |\mathcal{A}_t| = |\mathcal{A}_{t-1}| + |\mathcal{N}_{t-1}| - |\mathcal{R}_t|; \\ &\mathcal{J}_t = \mathcal{J}_{t-1} \cup \mathcal{I}_t \backslash \mathcal{N}_{t-1} \Rightarrow |\mathcal{J}_t| = |\mathcal{J}_{t-1}| - |\mathcal{N}_{t-1}| + |\mathcal{I}_t|; \\ &\mathcal{N}_t \subseteq \mathcal{D}_t \subseteq \mathcal{F}_t \subseteq \mathcal{J}_t \Rightarrow |\mathcal{N}_t| \le |\mathcal{D}_t| \le |\mathcal{F}_t| \le |\mathcal{J}_t|. \end{aligned}$$

Let $\Theta^{(t)}_{\mathcal{A},\mathcal{J}}(i,j)$ indicate the event that $S(t) = \{i,j\}$, *i.e.*, in time t, $|\mathcal{A}_t| = i$, and $|\mathcal{J}_t| = j$. The state transition probability $\Pr\big(\Theta^{(t)}_{\mathcal{A},\mathcal{J}}(i,j) \big| \Theta^{(t-1)}_{\mathcal{A},\mathcal{J}}(n,m)\big)$ for this two-dimensional

Markov chain can be obtained as follows:

$$\begin{aligned}
&\Pr\big(\Theta^{(t)}_{\mathcal{A},\mathcal{J}}(i,j)\big|\Theta^{(t-1)}_{\mathcal{A},\mathcal{J}}(n,m)\big)\\
=&\Pr\big(|\mathcal{N}_{t-1}|-|\mathcal{R}_t|=i-n,|\mathcal{N}_{t-1}|-|\mathcal{I}_t|=m-j\big|\Theta^{(t-1)}_{\mathcal{A},\mathcal{J}}(n,m)\big)\\
=&\sum_{k=0}^{k_0}\Pr\big(|\mathcal{N}_{t-1}|-|\mathcal{R}_t|=i-n,|\mathcal{N}_{t-1}|-|\mathcal{I}_t|=m-j,\\
&\qquad|\mathcal{N}_{t-1}|=k\big|\Theta_{\mathcal{A},\mathcal{J}}(n,m)\big)\\
=&\sum_{k=0}^{k_0}\Pr\big(|\mathcal{R}_t|=k+n-i\big||\mathcal{N}_{t-1}|=k,\Theta^{(t-1)}_{\mathcal{A},\mathcal{J}}(n,m)\big)\\
&\quad\times\Pr\big(|\mathcal{I}_t|=k+j-m\big||\mathcal{N}_{t-1}|=k,\Theta^{(t-1)}_{\mathcal{A},\mathcal{J}}(n,m)\big)\\
&\quad\times\Pr\big(|\mathcal{N}_{t-1}|=k\big|\Theta^{(t-1)}_{\mathcal{A},\mathcal{J}}(n,m)\big)\\
=&\sum_{k=0}^{k_0}\frac{\big(\mu T_f\big)^{k+n-i}\big(\lambda T_f\big)^{k+j-m}}{(k+n-i)!(k+j-m)!}e^{-(\mu+\lambda)T_f}\\
&\quad\times\Pr\big(|\mathcal{N}_{t-1}|=k\big|\Theta^{(t-1)}_{\mathcal{A},\mathcal{J}}(n,m)\big),
\end{aligned}\tag{6}$$

where $k_0=\min\{m,N-n\}$. Here, we assume $|\mathcal{I}_t|$ and $|\mathcal{R}_t|$ to independently follow the Poisson distribution with rate λ and μ, respectively. The second term in (6) can be written as

$$\begin{aligned}
&\Pr\big(|\mathcal{N}_t|=k\big|\Theta^{(t)}_{\mathcal{A},\mathcal{J}}(n,m)\big)\\
=&\sum_{p=k}^{m}\sum_{q=k}^{p}\Pr\big(|\mathcal{N}_t|=k,|\mathcal{D}_t|=q,|\mathcal{F}_t|=p\big|\Theta^{(t)}_{\mathcal{A},\mathcal{J}}(n,m)\big)\\
=&\underbrace{\sum_{p=k}^{m}\sum_{q=k}^{p}\Pr\big(|\mathcal{F}_t|=p\big|\Theta^{(t)}_{\mathcal{A},\mathcal{J}}(n,m)\big)}_{\mathrm{P}_0}\\
&\times\underbrace{\Pr\big(|\mathcal{D}_t|=q\big||\mathcal{F}_t|=p,\Theta^{(t)}_{\mathcal{A},\mathcal{J}}(n,m)\big)}_{\mathrm{P}_1}\\
&\times\underbrace{\Pr\big(|\mathcal{N}_t|=k\big||\mathcal{D}_t|=q,|\mathcal{F}_t|=p,\Theta^{(t)}_{\mathcal{A},\mathcal{J}}(n,m)\big)}_{\mathrm{P}_2}.
\end{aligned}\tag{7}$$

1) Calculation of P_0*:* Given n active appliances and m appliances which wish to join $\mathcal{A}_t$, $m-p$ appliances can not pass the power check, *i.e.*, their individual power request levels are greater than the remaining power budget. The probability that an appliance $i\in\mathcal{J}_t$ has its individual power request levels less than the remaining power budget is given by

$$\alpha_n\triangleq\Pr\Big(\mathcal{P}_i\le\mathcal{P}_{\max,t}-\sum_{j\in\mathcal{A}_t}\mathcal{P}_j\Big||\mathcal{A}_t|=n\Big)=\sum_{l_0=n+1}^{\lfloor\mathcal{P}_{\max,t}/\varepsilon\rfloor}\phi_\Sigma(n+1,l_0).$$

Thus, $\mathrm{P}_0=\binom{m}{p}\alpha_n^p(1-\alpha_n)^{m-p}$.

2) Calculation of P_1*:* Given p appliances, exactly p appliances' packets can be successfully received and $p-q$ appliances collide with each other when transmitting the PRM packets during the power request phase.

$$\begin{aligned}
\mathrm{P}_1&=\Pr\big(|\mathcal{D}_t|=q\big||\mathcal{F}_t|=p\big)\\
&=\underbrace{\Pr\big(p-q\text{ collisions}\big|q\text{ successes},|\mathcal{F}_t|=p\big)}_{\mathrm{P}_{10}}\\
&\quad\times\underbrace{\Pr\big(q\text{ successes}\big||\mathcal{F}_t|=p\big)}_{\mathrm{P}_{11}},
\end{aligned}\tag{8}$$

where $\mathrm{P}_{11}=\frac{w!}{w^q(w-q)!}$. Let h denote the number of successful power request packets sent among the remaining $p-q$ appliances given the conditions in P_{10}. Therefore, $\mathrm{P}_{10}=\Pr(h=0)=1-\Pr(h\ge1)$, where $h\ge1$ signifies that, among $p-q$ appliances' packets, at least one packet can be successfully received. Further, these packets can only choose a back-off value among $w-q$ numbers. Let G_i denote the event that the i-th appliance out of $p-q$ successfully transmits its packet given the conditions in P_{10}. Thus,

$$\begin{aligned}
\mathrm{P}_{10}&=1-\Pr(h\ge1)=1-\Pr\left(\bigcup_{i=1}^{p-q}G_i\right)\\
&=1-\sum_{j=1}^{p-q}(-1)^{j-1}\binom{p-q}{j}\frac{(w-q)!(w-q-j)^{p-q-j}}{(w-q)^{p-q}(w-q-j)!}.
\end{aligned}\tag{9}$$

3) Calculation of P_2*:* Given n active appliances and q appliances in $\mathcal{D}_t$, k appliances can be granted admission by the leader appliance. We employ random ACM to analyze the admission success probability, where, given $|\mathcal{D}_t|=q$, q steps may exist for admission control. The *admissible set* at the $(i+1)^{\text{th}}$ step is denoted $\mathcal{D}_t^{(i)}$. Initially, we have $\mathcal{D}_t^{(0)}=\mathcal{D}_t$. Fig. 3 shows the admission success probability given $|\mathcal{D}_t|=q$

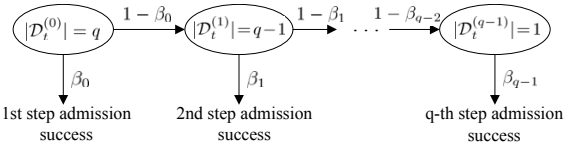

Fig. 3. Admission success probability given $|\mathcal{D}_t|=q$ and $|\mathcal{A}_t|=n$.

and $|\mathcal{A}_t|=n$. P_2 can be regarded as the admission success probability at the $(q-k+1)$-th step, and can be written as

$$\begin{aligned}
\mathrm{P}_2=&\Pr\big(|\mathcal{N}_t|=k\big||\mathcal{D}_t|=q,|\mathcal{A}_t|=n\big)\\
=&\Pr\big(\text{admission success}\big|\Psi_{\mathcal{A},\mathcal{D}}(n,q),\big|\mathcal{D}_t^{(q-k)}\big|=k\big)\\
&\times\Pr\big(\big|\mathcal{D}_t^{(q-k)}\big|=k\big|\Psi_{\mathcal{A},\mathcal{D}}(n,q)\big)\\
=&\beta_{q-k}\prod_{j=0}^{q-k-1}(1-\beta_j)
\end{aligned}\tag{10}$$

where $\Psi_{\mathcal{A},\mathcal{D}}(n,q)=\big\{|\mathcal{A}_t|=n,|\mathcal{D}_t|=q\big\}$. Given $\mathcal{D}_t^{(i)}$, the admission success probability β_i indicates the probability that the total request power level in $\mathcal{D}_t^{(i)}$ is less than the remaining power budget, *i.e.*,

$$\begin{aligned}
\beta_i&\overset{\text{def}}{=}\Pr\big(\text{admission success}\big||\mathcal{A}_t|=n,\big|\mathcal{D}_t^{(i)}\big|=q-i\big)\\
&=\sum_{l_0=q-i+n}^{\lfloor\mathcal{P}_{\max}/\varepsilon\rfloor}\phi_\Sigma(q-i+n,l_0),
\end{aligned}\tag{11}$$

$i=0,\cdots,q-2$ and $\beta_{q-1}=1$. Finally, given P_0, P_1 and P_2, we compute the state-transition probability given by (6).

C. Steady-state Distribution

Let $\pi_{n,m}\triangleq\lim_{t\to\infty}\Theta^{(t)}_{\mathcal{A},\mathcal{J}}(n,m)$ denote the steady-state distribution. For $(N+1)(N+2)/2$ states, the steady-state distribution vector is $\boldsymbol{\pi}\triangleq[\pi_{0,0},\pi_{0,1},\cdots,\pi_{N,0}]$. The steady-state distribution is obtained by solving $\boldsymbol{\pi}=\boldsymbol{\pi}\mathbf{P}$ and

$\boldsymbol{\pi}\mathbf{1}^T = 1$, where the state-transition probability matrix $\mathbf{P}$ is given by (6). The marginal PMF for $|\mathcal{A}_t|$ and $|\mathcal{J}_t|$ can be computed as: $\pi_n \triangleq \Pr\big(|\mathcal{A}_t| = n\big) = \sum_{m=0}^{N-n} \pi_{n,m}$; and $\pi_m \triangleq \Pr\big(|\mathcal{J}_t| = m\big) = \sum_{n=0}^{N-m} \pi_{n,m}$. For further analysis, we define the following probabilities:

$$\xi_p \triangleq \Pr\big(|\mathcal{F}_t| = p\big) = \sum_{n=0}^{N} \sum_{m=0}^{N-n} \pi_{n,m} \mathrm{P}_0, \tag{12}$$

$$\zeta_{n,q} \triangleq \Pr\big(|\mathcal{A}_t| = n, |\mathcal{D}_t| = q\big) = \sum_{m=0}^{N-n} \sum_{p=q}^{m} \pi_{n,m} \mathrm{P}_0 \mathrm{P}_1. \tag{13}$$

D. State-transition Diagram

Fig. 4 shows the state transition diagram of the protocol, for one arbitrary appliance i in the system. Six states are

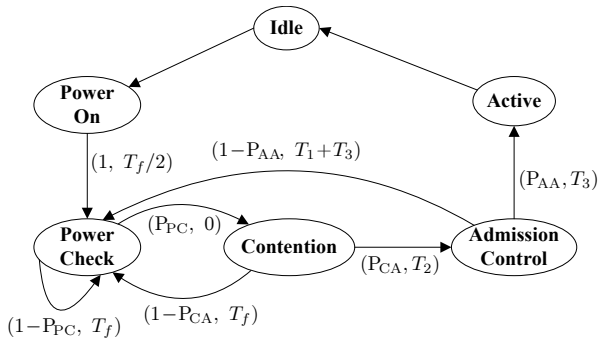

Fig. 4. State transition diagram for an arbitrary appliance.

considered for the appliance in this protocol, details of which are presented in [14].

E. State-transition Probability

We now compute the power check success probability ($\mathrm{P_{PC}}$), contention success probability ($\mathrm{P_{CA}}$) and admission success probability ($\mathrm{P_{AA}}$).

1) $\mathrm{P_{PC}}$*:* Power check success indicates that an appliance i perceives its power request level less than the remaining power budget, *i.e.*, this appliance is in the *feasible appliance set* $\mathcal{F}_t$. Then, the power check success probability $\mathrm{P_{PC}} \triangleq \Pr(i \in \mathcal{F}_t)$ is given by

$$\mathrm{P_{PC}} = \sum_{n=0}^{N} \Pr\big(|\mathcal{A}_t| = n\big) \cdot \Pr\big(a \in \mathcal{F}_t \big| |\mathcal{A}_t| = n\big) = \sum_{n=0}^{N} \pi_n \alpha_n. \tag{14}$$

2) $\mathrm{P_{CA}}$*:* Contention success indicates that no collisions happen when an appliance $i \in \mathcal{F}_t$ sends out the PRM packet and the *leader appliance* can receive it without errors, *i.e.*, this appliance is in the *admissible appliance set* $\mathcal{D}_t$. From (12), $\mathrm{P_{CA}} \triangleq \Pr(i \in \mathcal{D}_t)$ is given by

$$\begin{aligned} \mathrm{P_{CA}} &= \sum_{p=0}^{N} \Pr\big(|\mathcal{F}_t| = p\big) \times \Pr\big(\text{no packet collision} \big| |\mathcal{F}_t| = p\big) \\ &= \sum_{p=0}^{N} \xi_p \left(1 - \frac{1}{w}\right)^{[p-1]^+}, \end{aligned} \tag{15}$$

where $[x]^+ = \max[0, x]$.

3) $\mathrm{P_{AA}}$*:* Admission success indicates that the appliance $i \in \mathcal{D}_t$ can be granted admission by the *leader appliance*, *i.e.*, this appliance is in the *new active appliance set* $\mathcal{N}_t$. From (13), $\mathrm{P_{AA}} \triangleq \Pr(i \in \mathcal{N}_t)$ is given by

$$\begin{aligned} \mathrm{P_{AA}} =& \sum_{n=0}^{N} \sum_{q=0}^{N-n} \Pr\big(|\mathcal{A}_t| = n, |\mathcal{D}_t| = q\big) \\ & \times \Pr\big(a \in \mathcal{N}_t \big| |\mathcal{A}_t| = n, |\mathcal{D}_t| = q\big) \\ =& \sum_{n=0}^{N} \sum_{q=0}^{N-n} \zeta_{n,q} \left[\beta_0 + \sum_{i=1}^{q-1} \frac{q-i}{q-i+1} \beta_i \prod_{j=0}^{i-1} (1-\beta_j)\right]. \end{aligned} \tag{16}$$

F. Delay Analysis

We denote the average delay in the Power Check, Contention and Admission Control states as T_P, T_C and T_A, respectively. From the state-transition diagram (see Fig. 4), the average delay T_D is given by $T_\mathrm{D} = T_f/2 + T_\mathrm{P}$, where

$$T_\mathrm{P} = \mathrm{P_{PC}} T_\mathrm{C} + (1 - \mathrm{P_{PC}})(T_\mathrm{P} + T_f), \tag{17}$$

$$T_\mathrm{C} = \mathrm{P_{CA}}(T_2 + T_\mathrm{A}) + (1 - \mathrm{P_{CA}})(T_\mathrm{P} + T_f), \tag{18}$$

$$T_\mathrm{A} = \mathrm{P_{AA}} T_3 + (1 - \mathrm{P_{AA}})(T_\mathrm{P} + T_1 + T_3). \tag{19}$$

From (17) - (19), we have

$$T_\mathrm{D} = \frac{T_f}{2} + \frac{T_f - \mathrm{P_{PC}} \mathrm{P_{CA}} \mathrm{P_{AA}} T_1}{\mathrm{P_{PC}} \mathrm{P_{CA}} \mathrm{P_{AA}}}. \tag{20}$$

IV. Optimization of $\mathcal{P}_{\max,t}$ for EMC

In this section, we formulated an optimization problem that helps the EMC decide $\mathcal{P}_{\max,t}$. Specifically, we assume the EMC aims to minimize the total cost of electricity on a daily basis while considering variations in electricity prices and uncertainty of local wind power generation. We assume that the EMC has hourly day-ahead prices for the entire day and receives real-time prices several minutes before each hour.

A. Stochastic Feature of Wind Power

We use wind speed data from the National Renewable Energy Laboratory (Solar Radiation Research wing), which is located at latitude $39.742°$ North and longitude $105.18°$ West. The elevation is 1828.8 meters. The data are gathered during the following period: January 1st, 2009 to December 31st, 2009, with 10-minute sampling interval [16].

We model the stochastic behavior of wind power using the Markov Chain Monte Carlo (MCMC) technique, where the transition probability matrix is constructed from the historical wind speed data and wind turbine power curve. This matrix can be used to predict the wind power generation and aid in EMC scheduling framework. Given the wind speed, the power output of the wind turbine can be obtained from the power curves, which map the wind speed to wind turbine generation. For our model, we use the RAUM ENERGY™3.5kW wind turbine, and the instantaneous system power curve is shown in its data-sheet [17], where the wind power outputs form a set $\mathcal{H}$ with number of $|\mathcal{H}| = 11$ states, *i.e.*, $s_1, \ldots, s_{11}$ representing the $|\mathcal{H}|$ wind turbine generation values. For the first-order Markov Chain (FO-MC), the state evolution can be

described by the transition probability matrix $\mathbf{Q}$, whose entry q_{ij} represents the transition probability from state i at time $t-1$ to state j at time t, *i.e.*, $q_{ij} = \Pr\{X_t = j | X_{t-1} = i\}$, which is independent of time t. Second and third order Markov chains can also be used to describe the stochastic behavior. However, following the results in [18], these models provide approximately the same level of modeling accuracy as FO-MC. Thus, for simplicity in exposition, we choose FO-MC. Given the wind power data, q_{ij} can be estimated using the Monte Carlo method:

$$q_{ij} = \frac{n_{ij}}{\sum_{k \in \mathcal{H}} n_{ik}}, \tag{21}$$

where n_{ij} is the number of transitions from i to j encountered in the records. Fig. 5 shows the transition probability matrix $\mathbf{Q}$ obtained from the data. We notice that the diagonal and near-diagonal entries dominate, demonstrating the high auto-correlation of the wind power sequence.

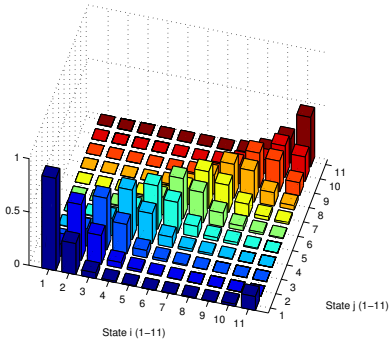

Fig. 5. Transition probability matrix of wind power

B. Problem Formulation

Given $\mathbf{Q}$ and the initial state s_{i0}, an estimate of the expected value of wind power at time t is given by

$$\tilde{W}_t = \sum_{j=1}^{|\mathcal{H}|} s_j \left[\mathbf{Q}^t\right]_{i0,j}, \tag{22}$$

where $[\mathbf{X}]_{i,j}$ indicates the entry with row i and column j in matrix $\mathbf{X}$. We formulate the optimization problem for the EMC at time t_0 with T-hour look ahead, K-min time slots in a rolling-based manner. Note that $T = 24$ is for daily optimization. For each time t, the EMC optimizes $\mathcal{P}_{\max,t}$ for $Z = 60T/K$ cycles from t_0, *i.e.*, $t \in [t_0+1, t_0+Z]$, with the predicted values of wind power $\tilde{W}_{t_0+1} \ldots \tilde{W}_{t_0+Z}$ using the actual wind power W_{t_0} as the initial state in (22). The problem can, therefore, be formulated as follows:

$$\begin{aligned} \min_{\mathcal{P}_{\max,t}} \quad & \sum_{t=t_0+1}^{t_0+Z} \kappa_t (\mathcal{P}_{\max,t} - \tilde{W}_t) \\ \text{s.t.} \quad & \mathcal{L}_t + \tilde{W}_t \le \mathcal{P}_{\max,t} \le \mathcal{U}_t + \tilde{W}_t, \\ & \sum_{t=t_0+1}^{t_0+Z} \mathcal{P}_{\max,t} \cdot \frac{K}{60} \ge \mathcal{E}_{t_0}. \end{aligned} \tag{23}$$

Here, κ_t is the electricity price with K-minute the interval. Since wind power data intervals and pricing signal updates are 10-minute and 1-hour, respectively, the optimization interval K can be chosen as 10 minutes. The price κ_t during the first hour after t_0 can be the real-time price (obtained several minutes before that hour). The following prices can either use the forecast hourly price as shown in [10], or the day-ahead price for approximation. $\mathcal{L}_t$ and $\mathcal{U}_t$ denote the lower and upper bounds, respectively, for power consumption level at time t. $\mathcal{E}_{t_0}$ denotes the minimum total power consumption for T hours horizon starting from t_0. These parameters can be determined by the EMC using learning algorithms that follow the consumer's usage patterns. Alternatively, we may select $\mathcal{L}_t$ as the aggregate power consumption level by real-time appliances, *i.e.*, $\mathcal{L}_t = \sum_{i \in \mathcal{V}_t} \mathcal{P}_i + \delta_t$, where $\mathcal{V}_t$ denotes the set of critical appliances at time t, while δ_t denotes the slack power level that corresponds to critical appliances with cycle power (*e.g.* air conditioners). Such a selection of $\mathcal{L}_t$ guarantees sufficient power budget to accommodate for real-time appliances. Additionally, $\mathcal{U}_t$ may be provided by the utility/aggregator to avoid aggregate peak power. We note that, with additional (predicted) wind power, the lower and upper bounds for $\mathcal{P}_{\max,t}$ are adjusted accordingly in (23).

V. Numerical Results

We assume the time frame length $T_f = 5$ min, where $T_1 = 4.5$ minutes, $T_2 = 29.9$s and $T_3 = 0.1$s. The beacon signal and each packet are 0.1s long, and thus the number of slots in the power request phase is $w = 298$ (not including the beacon signal). We consider L appliance types, and assume the power $\mathcal{P}_i = k\varepsilon$; $i = 1, \cdots, N$, $k = 1, \cdots, L$, which is uniformly distributed, *i.e.*, $p_k \triangleq \Pr(\mathcal{P}_i = k\varepsilon) = 1/L$. For simulations, we choose $L = 5$ and $\varepsilon = 100$W. For simplicity, we assume all L appliance types to have a duration of use that is exponentially distributed with mean $1/\mu$.

A. Delay Characteristics

We assume $\mathcal{P}_{\max,t} = \mathcal{P}_{\max}$ and a fixed arrival rate of λ for all hours. First, in Fig. 6, we plot the average delay as a function of $\mathcal{P}_{\max}$ for different (λ, μ) combinations. Results

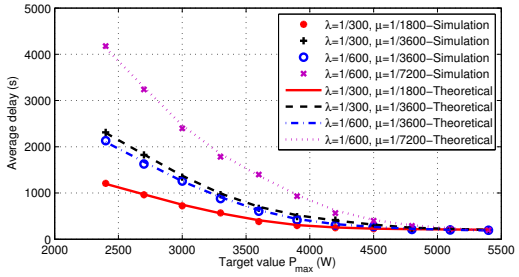

Fig. 6. Average delay versus $\mathcal{P}_{\max}$ with various (λ, μ) (Simulation and theoretical results). We choose random ACM and $N = 15$.

demonstrate that the average delay (i) decreases with increasing $\mathcal{P}_{\max}$; (ii) increases with appliance request (arrival) rate λ; and (iii) decreases with power usage complete (departure) rate μ. We also plot the theoretical average delay, given by (20), and see that it matches with the simulation results. We also note that, as $\mathcal{P}_{\max}$ increases beyond a certain value, *i.e.*,

when the total power consumption without scheduling is at most $\mathcal{P}_{\max}$, the average delay converges to the overhead of the protocol $\approx T_f/2 + T_2 + T_3 = 180s$. This can also be seen from (20) corresponding to $\mathrm{P_{PC}P_{CA}P_{AA}} = 1$.[2]

In Fig. 7, we plot the average delay as a function of the number N of appliances with different ACMs. We see that the average delay increases as N increases, since larger number of appliances cause more congestion. We also note that the average delays of the three ACMs are comparatively close to each other. From the plot we conclude that, since random ACM has linear implementation complexity, it can be considered to be a desirable option.

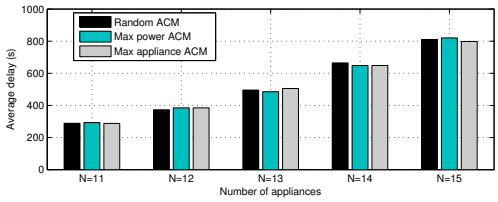

Fig. 7. Average delay versus N with various ACMs. In the simulations, we choose we choose $\mathcal{P}_{\max} = 3000$W, $\lambda = 1/900$, and $\mu = 1/3000$.

Fig. 8(a) shows the average delay versus the target power budget $\mathcal{P}_{\max}$ with different number of critical appliances in the system. We only present results for the random CCM policy as

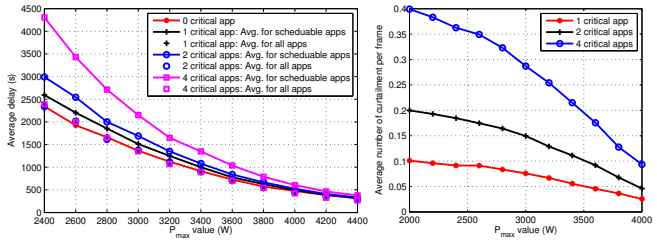

(a) Average delay with critical apps (b) Average curtailment per frame

Fig. 8. With critical appliances. In the simulations, we choose $N = 15$, $\lambda = 1/900$, and $\mu = 1/3000$.

the performance of other schemes matches closely with this. We see that with more critical appliances, the average delay for schedulable appliances become larger. This is primarily due to the fact that when one schedulable appliance is curtailed by the EMC/leader appliance, it needs to re-compete with other appliances to join the active set. When accounting for all appliances, it is interesting to note that the average delay is almost the same as the case of no critical appliance, indicating the presence of critical appliances will not increase the average delay in the system. Fig. 8(b) shows the average curtailment with different number of critical appliances. As expected, we see that with a larger number of critical appliances or smaller $\mathcal{P}_{\max}$, the average number of curtailment becomes larger.

B. Load Scheduling Results

We plot the power consumption of the proposed scheme using an optimized $\mathcal{P}_{\max,t}$ obtained from (23). We employ the price profile of 100 consecutive days as the day-ahead location marginal price (LMP) in the New York City zone from archival data $(09/01/2011 - 12/31/2011)$ of New York ISO [19]. Given the wind power data, the specified upper and lower bounds ($\mathcal{U}_t$, $\mathcal{L}_t$) and the total power consumption constraint ($\mathcal{E}_{t_0}$), the plot of the optimized $\mathcal{P}_{\max,t}$ for a day is shown in Fig. 9(c). For comparison, we also show the plot of $\mathcal{P}_{\max,t}$ which does not consider the wind power in Fig. 9(b), *i.e.*, $\tilde{W}_t = 0$ in the optimization problem (23). The wind power and electricity price profile for that day are

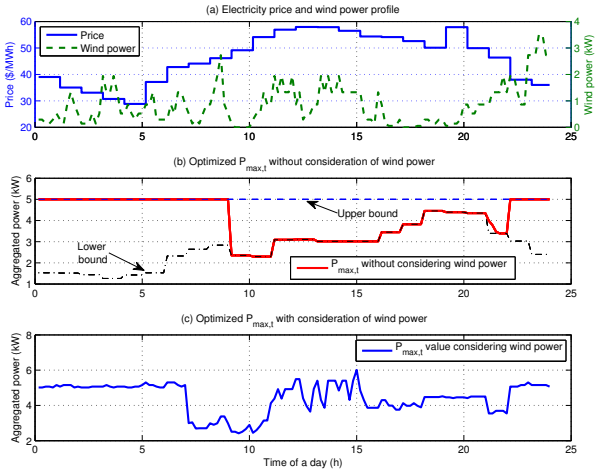

Fig. 9. Optimized power budget $\mathcal{P}_{\max,t}$ for a day.

shown in Fig. 9(a). The following comments are in order: (i) The optimization enables $\mathcal{P}_{\max,t}$ to be lower during high-price periods and vice versa, which improves the customers' savings in energy cost; (ii) during periods of wind power, $\mathcal{P}_{\max,t}$ is higher, which encourages customers to use the cheaper wind power, alleviating congestion in appliance access and thereby lowering average delay for each appliance.

We note that the benefits discussed above depend on how closely the actual demand using the proposed scheduling scheme approaches to the target value $\mathcal{P}_{\max,t}$. Fig. 10 shows the scheduling results of our scheme using the power budget obtained in Fig. 9. Here, we vary the mean arrival rate of appliances based on the time-of-day. Specifically, we assume an arrival rate of $\lambda = 1/1800$ during the hours $[1:7]$; $\lambda = 1/900$ during the hours $[8:17]$ and $[23:24]$; and $\lambda = 1/200$ during the hours $[18:22]$. We see that, for both the cases of with and without wind power, the scheduled total power consumption is below and close to the target value $\mathcal{P}_{\max,t}$. The proposed scheme enables powering-on of appliances to be scheduled as long as the power budget is available. Further, the max-power ACM guarantees the smallest gap between actual consumption and the target power $\mathcal{P}_{\max,t}$.

Next, in Fig. 11(a), we compare the cost of buying electricity from the grid over 100 days under the proposed scheme, and the non-scheduling policy; both policies consider the influence of wind power. We see that, with and without wind power the cost saving using the proposed scheme is 34.11% and 33.73%, respectively, better compared to the non-scheduling policy. The reason can be attributed to the fact that

[2]Since the number N of appliances is not large, the PRM packet receiving probability $\mathrm{P_{CA}} \approx 1$.

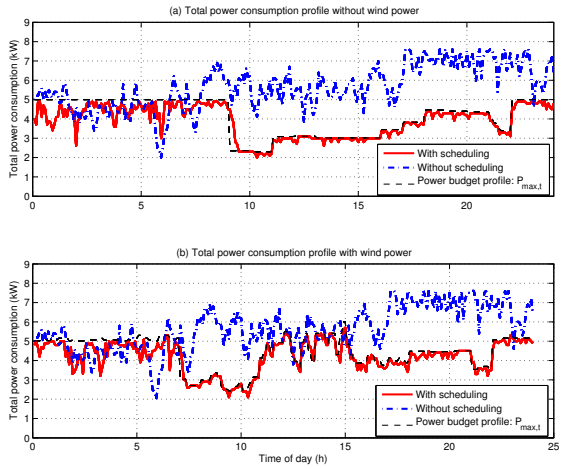

Fig. 10. Total power consumption under our scheme using $\mathcal{P}_{\max,t}$ in Fig. 9 with/without wind power. Unscheduled power consumption for benchmark. In the simulations, we choose $N = 25$, $\mu = 1/3600$ and random ACM.

optimized $\mathcal{P}_{\max,t}$ values encourage power usage during low price periods, and the proposed protocol enables appliances to make the best effort to approach the target without exceeding it. We also see that wind power integration can further lower the cost by about 7.39% under our scheme, demonstrating the benefits of using distributed renewable energy at the residential level. The saving is further increased when wind power accounts for a larger portion of the overall supply in-home.

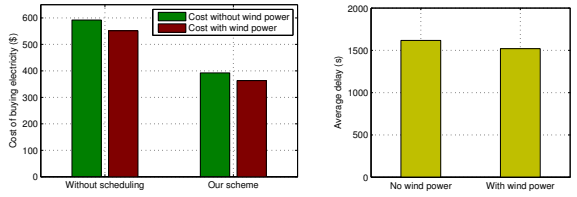

(a) Cost comparison (b) Average delay comparison

Fig. 11. Comparison of (100-day total) cost for buying electricity from the grid under our scheme and non-scheduling benchmark, for both with and without wind power, and (100-day) average delay under wind power influence. Simulation parameters are the same with that in Fig. 10.

Lastly, Fig. 11(b) compares the average delay of our scheme with and without consideration of the wind power. We see that, the average delay with wind power is slightly lower (6%) than that without wind power. This is because the optimized $\mathcal{P}_{\max,t}$ can be larger at the time when there is wind power; larger power budget incurs less congestion and lower average delay.

VI. Conclusion

In this paper, we proposed a joint access and scheduling scheme for appliances operating over a consumer-premise communication network. The scheme could be incorporated in various DR schemes, such as smart pricing-based or DLC-based. The scheme considers both schedulable appliances, whose powering-on can be delayed, and critical appliances that require real-time power usage. We modeled the evolution of the protocol as a two-dimensional Markov chain and derived the average delay of an arbitrary appliance. We formulated an optimization problem for the EMC, enabling it to compute the target power level for the home while incorporating effects of price variations and local wind power uncertainty. Simulations verified the analysis and showed that the proposed scheme lowers electricity costs for customers.

References

[1] U.S. Department of Energy, "The Smart Grids: An introduction," 2009. [Online]. Available: http://energy.gov/oe/downloads/smart-grid-introduction-0

[2] Federal Energy Regulatory Commission (FERC), "Order No. 719, Wholesale Competition in Regions with Organized Electric Markets," October 2008. [Online]. Available: http://www.ferc.gov/whats-new/comm-meet/2008/101608/E-1.pdf

[3] ——, "Order No. 745, Demand Response Compensation in Organized Wholesale Energy Markets," March 2011. [Online]. Available: http://www.ferc.gov/EventCalendar/Files/20110315105757-RM10-17-000.pdf

[4] M. Alizadeh, A. Scaglione, and R. Thomas, "From packet to power switching: Digital direct load scheduling," *IEEE Journal on Selected Areas in Communications (JSAC): Smart Grid Communications Series, to appear*, 2012.

[5] CNT Energy and Ameren Illinois Utilities, "Ameren Power Smart Pricing," 2012. [Online]. Available: http://www.powersmartpricing.org/how-it-works/

[6] CNT Energy and ComEd Utilities, "ComEd Residential Real-Time Pricing (RRTP)," 2012. [Online]. Available: http://www.cntenergy.org/pricing/comed-rrtp/

[7] Solar Direct, "U.S. Small Wind Tax Credit." [Online]. Available: http://www.solardirect.com/rebates/wind_skystream.html

[8] ——. [Online]. Available: http://www.solardirect.com/rebates/wind_skystream.html

[9] S. Kishore and L. Snyder, "Control mechanisms for residential electricity demand in smartgrids," in *Proc. of IEEE Conf. on Smart Grid Communications*, 2010.

[10] A. Mohsenian-Rad, V. Wong, J. Jatskevich, R. Schober, and A. Leon-Garcia, "Autonomous demand side management based on game-theoretic energy consumption scheduling for the future smart grid," *IEEE Trans. on Smart Grid*, vol. 1, no. 3, pp. 320–331, 2010.

[11] D. L. Ha, M. H. Le, and S. Ploix, "An approach for home load energy management problem in uncertain context," *Proc. of IEEE International Conference on Industrial Engineering and Engineering Management*, pp. 336–339, 2008.

[12] P. Samadi, H. Mohsenian-Rad, R. Schober, V. Wong, and J. Jatskevich, "Optimal real-time pricing algorithm based on utility maximization for smart grid," in *Proc. of IEEE Conf. on Smart Grid Communications*, 2010.

[13] G. Xiong, C. Chen, S. Kishore, and A. Yener, "Smart (In-Home) Power Scheduling for Demand Response on the Smart Grid," in *Proc. of IEEE PES Innovative Smart Grid Technologies (ISGT)*, Anaheim, CA, 2011.

[14] C. Chen, K. Nagananda, G. Xiong, S. Kishore, and L. Snyder, "Analysis of a Joint Access and Scheduling Scheme for Residential Energy Management Controller," in *7th IEEE Sensor Array and Multichannel Signal Processing Workshop (SAM): Special Session on Smart Grids*, invited paper, to appear, 2012.

[15] H. Kellerer, U. Pferschy, and D. Pisinger, *Knapsack Problems*. Berlin: Springer, 2004.

[16] Custom monthly wind speed data. NERL Solar Radiation Research Laboratory. [Online]. Available: http://www.nrel.gov/midc/srrl_bms

[17] 3.5 kw wind turbine system specification sheet. Raum Energy. [Online]. Available: http://www.raumenergy.com/turbine3kw.html

[18] G. Papaefthymiou and B. Klockl, "MCMC for wind power simulation," *IEEE Transactions on Energy Conversion*, vol. 23, no. 1, pp. 234–240, 2008.

[19] New York ISO, "New York ISO Day-ahead Locational-Based Marginal Price (LBMP)-Zonal, Archive." [Online]. Available: http://mis.nyiso.com/public/P-2Alist.htm